Review Article

phys. stat. sol. (b) **118**, 463 (1983)

Subject classification: 6 and 20.1; 22.1.1; 22.1.2

Xerox Palo Alto Research Center[1])

Vibrational Spectra of Hydrogen in Silicon and Germanium

By

M. Cardona[2])

Contents

1. Introduction

The vibrational spectra of Si-H and Ge-H bonds in amorphous silicon (a-Si) and germanium (a-Ge) have been the object of considerable study [1 to 8]. This interest has been triggered, in part, by the role of hydrogen in passivating dangling bonds in the amorphous materials. Si–H bonds have also been studied on c-Si surfaces [9] and in the bulk of c-Si [10 to 15]. Three groups of structures are found in the infrared and Raman spectra. They correspond respectively to bond stretching vibrations of the Si–H(Ge–H) bonds, in the 1900 to 2150 cm^{-1} region, bond bending vibrations of SiH_2 and SiH_3 radicals at 840 to 910 (750 to 870) cm^{-1} and bond wagging vibrations around 650 cm^{-1}. Beside these modes one also observes a broad low frequency spectrum (0 to 550 cm^{-1} in a-Si, 0 to 300 cm^{-1} in a-Ge) which corresponds to the vibrations of the network of Si–Si(Ge–Ge) bonds [16 to 20]. The ir spectra also show a rather sharp

---

[1]) 3333 Coyote Hill Road, Palo Alto, California 94304, USA.

[2]) Permanent address: Max-Planck-Institut für Festkörperforschung, Stuttgart, FRG.

structure at 210(120) cm^{-1} which is particularly strong whenever hydrogen is present and depends on the hydrogen concentration. It is probably related to vibrations of the Si–Si bonds in $\mathrm{HSi{-}Si_3}$ units, where the first silicon is attached to a hydrogen [6, 16]. The vibrations of the Si–Si bonds are easily distinguished from those of Si–H bonds by measuring deuterated Si(Si–D). The latter lower their frequency approximately like the factor $2^{-1/2}$ while the former (Si–Si bonds) do not change for the deuterated material.

While there is general agreement about the gross features of these three groups of bands, a number of discrepancies and contradictions in the interpretation of the substructure of these bands remains. For a-Si, for instance, the stretching bands show substructure at 2000, 2100, and 2140 cm^{-1}, generally attributed to SiH, $\mathrm{SiH_2}$, and $\mathrm{SiH_3}$ groups, respectively. However, a contribution to the 2100 band due to Si–H radicals is believed to exist sometimes also [5, 6, 21]. Moreover, the Si–H bonds at c-Si [111] surfaces give a stretching mode at 2080 cm^{-1}, higher than in the bulk of a-Si. The bond stretching spectrum of the Si–H bonds in the bulk of c-Si exhibits a large number of very sharp lines [10 to 15] whose relationship to the corresponding spectra of a-Si and the c-Si surfaces is not well understood. While the interpretation of the strong wagging band at ≈ 640 cm^{-1} seems to be clear, there exists considerable uncertainty as to the bending modes, which have up to four components for a-Si in the 800 to 900 region [2, 4].

The purpose of this paper is to give a comprehensive discussion of the vibrational spectra of hydrogen (or deuterium) in a-Si, c-Si, and c-Si surfaces and in a-Ge. In Section 2 we present a simple valence force field model for the vibrational frequencies of Si–H bonds. In Section 3 we discuss the observed vibrational spectra in the light of the results of Section 2 and by comparison with the spectra of polysilanes and cyclopolysilanes. We also discuss the strength of the absorption lines. It enables us to retrieve the concentration of Si–H bonds in the various coexisting species. Section 4 presents a similar, although less complete discussion for a-Ge.

2. Vibrational Frequencies of SiH_n and GeH_n: Valence Force Field Model

The analysis of Clark and Weber [22] of the vibrational frequencies of disilane ($\mathrm{Si_2H_6}$) and related compounds in terms of valence force field constants suggests a similar analysis for the $\mathrm{SiH}_n(\mathrm{GeH}_n)$ radicals under consideration. Those authors include a stretch–stretch force constant f_DD for the Si–H bond, and bond bending constants f_AA and f_BB for the H–Si–H and the H–Si–Si bonds, respectively. For $\mathrm{Si_2H_6}$ $f_\mathrm{AA} \approx f_\mathrm{BB}$ within error. They differ by $\approx 8\%$ for $\mathrm{Ge_2H_6}$. We shall assume for simplicity that these force constants are equal. All other cross coupling force constant, such as stretch–bend f_DA, bend–bend f_AB, etc. are negligible for our purpose ($\leqq 1\%$ of f_DD). The only significant cross coupling force constant is f_DB which amounts to 10% of f_DD. This constant produces some coupling between the bending–wagging and the stretching modes but can also be neglected to first order.

2.1 Vibrations of $\mathrm{SiH_4}$

For the sake of completeness we start by giving the four vibrational frequencies of the tetrahedral silane (germane) molecules as a function of the force constants f_AA and f_DD [23]:

$$\begin{aligned} m\omega_1^2 &= f_\mathrm{DD}\,, \\ m\omega_2^2 &= 3f_\mathrm{AA}\,, \\ m(\omega_3^2 + \omega_4^2) &= f_\mathrm{DD}(1 + 4m/3M) + 2f_\mathrm{AA}(1 + 8m/3M)\,, \\ m^2\omega_3^2\omega_4^2 &= 2f_\mathrm{DD}f_\mathrm{AA}(1 + 4m/M)\,, \end{aligned} \tag{1}$$

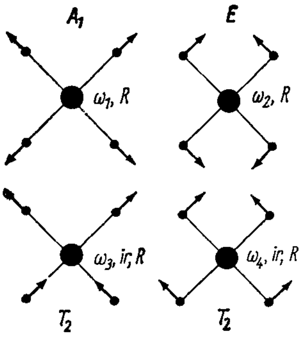

Fig. 1. Schematic diagram of the four vibrational modes of SiH_4 assuming $M \gg m$. The figure represents the projection on a [100] plane with the bonds along the ⟨111⟩ directions

where m is the atomic mass of hydrogen (deuterium) and M that of Si(Ge). The frequencies $\omega_1 - \omega_4$ have the symmetries A_1, E, T_2, and T_2, respectively (point group T_d, see Fig. 1); ω_3 and ω_4 are coupled in general but become decoupled in the case $m \ll M$. This approximation is very good for Ge and fair for Si. We shall use it here throughout for the sake of simplicity. It leads to

$$m\omega_3^2 = f_{DD}\,, \qquad m\omega_4^2 = 2f_{AA}\,. \tag{2}$$

From the experimental values $\omega_1 = 2186\ \text{cm}^{-1}$ [24, 25] we find for SiH_4 with (1) $f_{DD} = 2.82 \times 10^5$ dyn/cm in reasonably good agreement with the value given in [22] for Si_2H_6 ($f_{DD} = 2.71 \times 10^5$ dyn/cm). From the experimental value $\omega_2 = 972\ \text{cm}^{-1}$ for SiH_4 we find, with (1) $f_{AA} = 1.86 \times 10^4$ dyn/cm, also in good agreement with [22] ($f_{AA} = 1.88 \times 10^4$ dyn/cm). These facts support the transferability of these force constants for the calculation of the vibrations of Si–H bonds in a-Si. Similar facts hold for GeH_4, Ge_2H_6, and Ge–H bonds [22].

2.2 *Vibrations of SiH_2*

2.2.1 *Stretching modes*

The SiH_2 group has C_{2v} point group symmetry. The stretching vibrations split into a symmetric and an asymmetric mode (A_1, B_1, Fig. 2), both infrared and Raman active. If additivity of dynamical charges for the two bonds is assumed, the B_1 mode should be twice as strong in ir absorption as A_1 for a tetrahedral bond angle of 109°. Likewise, under the assumption of polarized scattering, which usually applies to stretching modes of *covalent bonds*, only the A_1 mode should show Raman activity. Within the model of f_{DD} and f_{AA} force constants the frequencies of both stretching modes are degenerate and should coincide with that of the ω_1 mode of SiH_4.

The most reliable measurement of the vibrational frequencies of SiH_2 radicals is obtained from the spectra of cyclopolysilanes (cyclopentasilane $(SiH_2)_5$ [26] and cyclohexasilane $(SiH_2)_6$) [27]. In these molecules the Si–H bonds appear only as SiH_2 combinations and there are no complications associated with the overlap and/or interaction with SiH and SiH_3 groups. The stretching modes of $(SiH_2)_5$ are centered at $2132\ \text{cm}^{-1}$ with a splitting of $5\ \text{cm}^{-1}$; those of $(SiH_2)_6$ at 2124 with a splitting of $8\ \text{cm}^{-1}$. The average frequency of these stretching modes $\approx 2128\ \text{cm}^{-1}$ is lower than that found for SiH_4. This has been attributed [2, 28, 29] to the varying electronegativity of the atoms or radicals attached to the Si. A linear inter-extrapolation between $2186\ \text{cm}^{-1}$ for SiH_4 and $2128\ \text{cm}^{-1}$ for $(Si)_2$–SiH_2 yields $2157\ \text{cm}^{-1}$ for Si–SiH_3, in good agreement with measurements for disilane [30] and $2099\ \text{cm}^{-1}$ for $(Si)_3$–SiH.

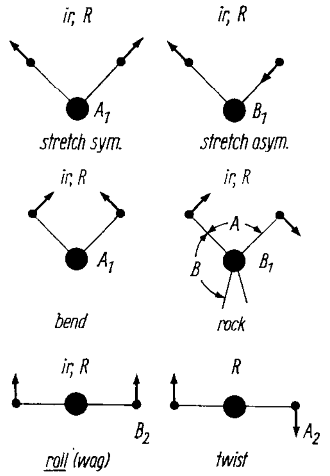

Fig. 2. Schematic diagram of the vibrations of $SiH_2(GeH_2)$ radicals (C_{2v} point group)

The splitting of the stretching A_1 and B_1 modes lies, as mentioned, between 5 and 8 cm^{-1}. From the fact that the lower frequency component is more strongly infrared active than the upper one, which is Raman active, we infer that it corresponds to the asymmetric B_1 mode. The A_1–B_1 stretch splitting is produced, in part, by the f_{DB} force constant which couples the A_1 stretch with the A_1 bend mode (see Fig. 2 and below), and similarly the corresponding B_1 modes.

2.2.2 *Angular modes*

Each one of the bonds in SiH_2 has two angular degrees of freedom. They can be combined into the four symmetry adapted modes (C_{2v} group) of Fig. 2. We designate them with the pictorial names of bending (A_1 symmetry), rocking (B_1), rolling (B_2), and twisting (A_2). The rolling mode is usually also called wagging mode. We reserve here the term wagging for the analog modes of SiH and SiH_3. The term "rolling" is less ambiguous in the case of SiH_2.

The four "angular" modes of Fig. 2 are Raman active while only the bending, rocking, and rolling modes are ir active. In order to derive the frequencies of these modes we note that the A_1 (bend) mode can be obtained as linear combination of the E and $T_2(\omega_4)$ modes of Fig. 1:

$$|A_1\rangle = 2^{-1/2}[|E\rangle + |T_2\rangle] \,. \tag{3}$$

Hence using equations (1) and (2) we obtain for the frequency of this mode

$$m\omega^2(A_1) = (5/2)\, f_{AA} \,. \tag{4}$$[3]

The effective force constant $(5/2)\, f_{AA}$ of (4) has two contributions. One of them arises from the H–Si–H angular force constant f_{AA}, the others from the H–Si–Si force constant f_{BB} which has been assumed to be equal to f_{AA}. It is easy to see that the H–Si–H forces contribute an amount $2f_{AA}$ to equation (4). Hence the H–Si–Si force must contribute $(1/2)\, f_{BB} \approx (1/2)\, f_{AA}$. (4) can thus be written more generally

$$m\omega^2(A_1) = 2f_{AA} + (1/2)\, f_{BB} \,. \tag{5}$$

---

[3] Note that the definition of f_{AA} is that of [22]. It differs by a factor of r/d from that of [32], where r and d are the lengths of the Si–Si and Si–H bonds, respectively.

The frequency of the B_1 (rocking) mode of Fig. 2 follows immediately from (5) if one considers that for this mode the f_{AA} contributions is absent but that of f_{BB} is the same as in (5). We find

$$m\omega^2(B_1) = (1/2)\, f_{BB} \approx (1/2)\, f_{AA}\,. \tag{6}$$

The frequencies of the B_2(roll) and A_2(twist) modes are easily obtained by considering that within our model they are degenerate. The A-angle between the H–Si–H bonds varies only quadratically with the atomic displacements of these modes and hence the frequencies of these modes are the same as if *only one atom would move* (see vibrations of SiH in Section 2.3). Their degeneracy thus follows. The frequency of vibration of one single Si–H bond is easily obtained from equation (5) by dividing by two the f_{AA} contribution, thus

$$m\omega^2(B_2) = m\omega^2(A_2) \approx f_{AA} + \tfrac{1}{2}\, f_{BB} \approx \tfrac{3}{2}\, f_{BB}\,. \tag{7}$$

The frequencies of the angular modes of SiH_2 calculated with the average force constants $f_{AA} \approx f_{BB} \approx 1.86 \times 10^4$ dyn/cm of [22] are given in Table 1.

Table 1

Vibrational frequencies of Si–H_2 bands (in cm^{-1}) calculated as described in the text. Also, in brackets, experimental values which come closest to the conditions of the calculation

SiH	stretch A_1 2099 (2080) [9]	wag E 685 (630) [9]				
SiH_2	A_1, B_1 2128 (2128) [26, 27]	roll B_2 685 (625—720) [26, 27]	twist A_2 685 (655) [26, 27]	bend A_1 885 (897) [26, 27]		rock B_1 395 (380 ?) [26, 27]
SiH_3	A_1, E 2157 (2167) [22, 30] (2153) [22, 30]	wag E 505 (502) [22, 30]	—	bend A_1 791 (876) [22, 30]	bend E 911 (936) [9]	twist A_1 100
SiH_4	A, T_2 2186 (2186) [51] (2189) [51]	—	—	bend E 969 (972) [51]	bend T_2 791*) (913) [51]	

*) Obtained with equation (2). Agreement with experiment improves considerably if equation (1) is used.

2.3 Vibrations of SiH

The vibrational frequencies of single Si–H bonds, with the Si implicitly assumed tied to the other Si atoms or atoms of similar electronegativity, follow automatically from the discussion in Section 2.2. The point group in the case of three Si atoms tied to the Si, and/or of an amorphous background assumed rotationally invariant, is C_{3v}: the stretching mode has A_1 symmetry (ir and Raman active). Its frequency was estimated in Section 2.2 to be 2089 cm^{-1}. It agrees reasonably well with the vibrational frequency of H adsorbed on (111) Si surfaces (2080 cm^{-1}) [9]. The angular (wagging) modes are twofold degenerate (E symmetry, ir and Raman active). Their frequency is the same as that given in equation (7).

2.4 Vibrations of SiH_3

We also assume that the Si atom is attached to another Si (or an atom of similar electronegativity) and a completely isotropic background. The point group is, like for SiH, C_{3v}. There are now, however, three stretching modes which split into a singlet A_1 and a doublet E. Under the assumptions of a nearly static effective charge and an isotropic Raman polarizability, only the A_1 mode is Raman active while the E-mode is more strongly ir active than A_1.

The *average* frequency of the A_1–E stretching modes has been estimated in Section 2.2 to be 2157 cm^{-1}. The A_1–E splitting can be obtained by averaging the odd and even components of A_1 and E in disilane. Note that this molecule has inversion symmetry while our SiH_3 group does not. We find in this manner from [22] $\omega(A_1) = 2153$, $\omega(E) = 2167$ cm^{-1}. In this case the *symmetric* (A_1) mode is lower than the non-symmetric one (E), contrary to what happens for SiH_2 (see Section 2.2.1).

There are for SiH_3 six angular modes. They split into two E modes (bend and wag, see Fig. 3), an A_1 bending mode and a twisting mode of A_2 symmetry. The latter is ir and Raman forbidden. All others are ir and Raman *symmetry* allowed. We point out first that the frequency of the A_2 twisting mode is zero within our simple force constants model as it corresponds to a rigid rotation of the SiH_3 radical. The corresponding mode has been estimated to be at 144 cm^{-1} for Ge_2H_6 (digermane) [30] as a result of residual force constants. We would therefore expect it to lie at ≈ 150 cm^{-1} for Si_2H_6. Since, in this case it corresponds to a rigid rotation of one (SiH_3) unit with respect to the other, the twisting frequency for the SiH_3 radical attached to a Si matrix should be at about $150 \times 2^{-1/2} \approx 100$ cm^{-1}.

The calculation of the frequencies of the bending and wagging E-modes is somewhat more involved. These modes are coupled because of the fact that they have the same symmetry. Hence the diagrams of Fig. 3 for these modes do not represent their exact

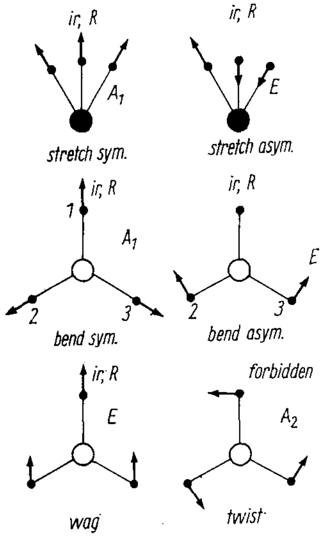

Fig. 3. Schematic diagram of the vibrations of the $SiH_3(GeH_3)$ radicals (C_{3v} point group)

eigenvectors. The vibrational frequencies are obtained by diagonalizing the matrix M (see [22])

$$M = G \times F \,,$$
$$G = m^{-1}\begin{pmatrix} 5/2 & 1/2 \\ 1/2 & 1 \end{pmatrix}; \qquad F = \begin{pmatrix} f_{AA} & 0 \\ 0 & f_{BB} \end{pmatrix}. \tag{8}$$

These matrices are readily obtained from Table 1 in [22]. The diagonalization leads to (we take as usual $f_{AA} \approx f_{BB}$):

$$m\omega_E^2(\text{wag}) = f_{AA}([7 - \sqrt{13}]/4) = 0.88 f_{AA} \,,$$
$$m\omega_E^2(\text{bend}) = f_{AA}([7 + \sqrt{13}]/4) = 2.65 f_{AA} \,, \tag{9}$$

the frequencies calculated with (9) and the f_{AA} of [22] are listed in Table 2.

Table 2

Vibrational frequencies of Ge–H bands (in cm^{-1}) calculated as described in the text. Also, in brackets, experimental values which come closest to the conditions of the calculation

GeH	stretch A_1 1994	wag E 664				
GeH_2	A_1, B_1 2036	roll B_2 664	twist A_2 664	bend A_1 858		rock B_1 380
GeH_3	A_1, E 2078 (2072) [22] (2082) [22]	wag E 490 (466) [22]	—	bend A_1 767 (794) [22]	bend E 883 (880) [22]	twist A_1 ≈ 100
GeH_4	A, T_2 2120 (2111) [51] (2189) [51]	—	—	bend E 931 [51]	bend T_2 821 [51]	

For the sake of completeness we list in Table 2 the vibrational frequencies of GeH_n radicals calculated in the same manner as those of Table 1 with the restoring force constant [22] $f_{AA} \approx f_{BB} = 1.75 \times 10^4$ dyn/cm.

3. Vibrational Spectra of SiH_n ($n = 1, 2, 3$) in Solids

3.1 *Surfaces*

The vibrational spectra of hydrogen adsorbed on a Si[111] surface has been investigated by means of infrared absorption and by electron energy loss spectroscopy [9]. Energy loss spectroscopy yields a bond stretching peak at 2080 cm^{-1} for low coverage, which shifts to about 2140 cm^{-1} at high coverage. Infrared absorption, although less sensitive, gives similar results: a peak at 2060 cm^{-1} which shifts to ≈ 2110 cm^{-1} with increasing coverage. We believe the 2080 peak corresponds to single Si–H bonds at the surface while the higher frequency peak corresponds to SiH_3 groups. These frequencies agree well with the predictions of Table 1 provided a downward shift of $\approx 20\ \mathrm{cm}^{-1}$ is subtracted from the predicted frequencies. Such shift would be qualitatively expected as a result of the polarization of the Si crystal by the vibration. We shall see in Sections 3.2 and 3.3 that a larger down shift ($\approx 100\ \mathrm{cm}^{-1}$) occurs when the Si–H bonds are imbedded in the *bulk* of the solid.

Electron energy loss spectroscopy [9] also shows a bond wagging band at 630 to 640 cm^{-1} and a bond bending feature at 900 cm^{-1}. The bond bending peak is likely to be the low frequency (A_1) component of the A_1–E bond bending doublet of SiH_3 which is more strongly ir active than the E-component [30].

3.2 a-Si

The bond stretching peak of SiH in the bulk of a-Si occurs at 2000 cm^{-1} [2 to 5], see Table 3. It is therefore shifted down by about 100 cm^{-1} with respect to the predicted frequency of Table 1 and by $\approx 80\ \mathrm{cm}^{-1}$ with respect to the frequency of Si–H bonds on [111] Si surfaces. It is easy to account for this shift in terms of the depolarizing field produced by the vibrating dipole in a cavity inside the solid. Under the assumption of a spherical cavity of radius R the corresponding frequency shift can be easily calculated to be [31]

$$\Delta\omega = -\,[e^{*2}/(2mR^3\omega)]\,[(\varepsilon - 1)/(2\varepsilon + 1)]\,, \tag{10}$$

where e^* is the dynamical charge of the dipole and $\varepsilon \approx 12$ the dielectric constant of the a-Si matrix. Taking $e^* \approx 0.4\,e$, a reasonable value (see [24] and also Section 3.4), and R equal to the covalent radius of Si (i.e., we assume that the Si–H bond is located in a vacancy), we calculate with (10) $\Delta\omega \approx -80\ \mathrm{cm}^{-1}$, in excellent agreement with the considerations above. We note that as the hydrogen concentration increases ε will decrease and a slight up-shift of the vibrational frequency should be expected. Such shifts are sometimes observed. Clearer evidence for these "solid state" shifts is observed for the SiH stretching modes of a-C_xSi_{1-x}(H) with increasing C concentration (i.e., with decreasing ε) [31].

An absorption peak is usually observed at $\approx 2100\ \mathrm{cm}^{-1}$ for samples with relatively high H concentration ($\gtrsim 10\%$) [2 to 7]. It is usually accompanied by bands in the 850 to 900 cm^{-1} region which, according to Table 1, correspond to bond bending modes of SiH_2. The 2100 cm^{-1} peak is thus usually assigned to the bond stretching vibrations (A_1, B_1) of SiH_2 radicals. It is shifted by $\approx 28\ \mathrm{cm}^{-1}$ from the prediction of

Table 3
Vibrational frequencies (in cm^{-1}) of structures observed in the infrared and Raman spectra of a-Si:H related to the presence of hydrogen

	SiH	SiH_2	SiH_3
bond	2000 (A_1)	2100 (A_1)	2140 (A_1, E)
stretching	2085 (A_1)	2090 (B_1)	
bond	—	870 (A_1)	
bending		890 $(SiH_2)_2$ 840 $(SiH_2)_2$	910 (E) 860 (A_1)
wag, roll	640 (E)	640 (A_2, B_2)	—
Si_3–SiH	210	210	

Table 1. Hence one may conclude that it corresponds to SiH_2 radicals at the inner surfaces of voids or of cavities larger than the single vacancy just discussed. We should point out, however, that as discussed in Section 3.4 and in [6], the dynamical charge for the SiH_2 stretching vibrations is much smaller than for SiH. Thus we would expect the shift of (10) to be rather small for SiH_2 and the frequency of the stretching mode of this group to be at $\approx 2100\ cm^{-1}$ regardless of the size of the cavity.

The A_1–B_1 splitting of this mode in SiH_2 should be between 5 and 10 cm^{-1} [26, 27], too small to be resolved in view of the measured linewidths ($\approx 50\ cm^{-1}$). We have, however, mentioned in Section 2.2 that the upper B_1 mode should be mainly Raman active while the A_1 mode should be ir active. The stretching modes of SiH_2 are sometimes observed around $\approx 2090\ cm^{-1}$ in ir spectra and at $\approx 2100\ cm^{-1}$ in Raman. This may indeed be an indication of the A_1–B_1 splitting.

The rather simple picture just presented is marred by the fact that sometimes a peak or a component of the bond stretching band centered at 2100 cm^{-1} is observed without the 850 to 900 cm^{-1} bond bending counterpart [5 to 7, 21]. The simplest interpretation of this structure is based on (10) and the assumption that one has SiH bonds in larger cavities ($R \geqq 2$ Å suffices) or in macroscopic voids. The amount of this component is usually enhanced upon annealing at ≈ 400 °C (see Fig. 6 of [5]), a fact which may be accounted for by the formation of larger voids at these temperatures as a result of structural relaxation. We point out that an electronegativity induced shift from 2000 to $\approx 2100\ cm^{-1}$ would also be expected for O=Si—H groups [32]. The authors of [5] and [6], however, believe that their samples were free of oxygen. The existence of the $\approx 2100\ cm^{-1}$ band of SiH has been confirmed in a recent publication by Dellafera et al. [33]. These authors were able to prepare by evaporation in a molecular hydrogen atmosphere a-Si:H which exhibits an absorption peak at 2085 cm^{-1} and no bond bending bands. The ir spectra of these films, however, show traces of oxygen contamination.

The presence of SiH_3 groups in heavily hydrogenated a-Si was postulated by Brodsky et al. [2] in order to explain a shoulder in the bond stretching bands at 2120 cm^{-1}. Work by Lucovsky et al. [4] on samples deposited on a low temperature substrate ($T_s \approx -125$ °C) confirmed this conjecture as they found a well defined peak at 2140 cm^{-1} both in ir and Raman spectra (see Fig. 6 of [4]). According to Table 1 this peak should occur at 2157 cm^{-1}; we may therefore assume it is down-shifted by the typical amount ($\approx 20\ cm^{-1}$) associated with groups in "large" voids.

The least controversial of the vibrational modes of SiH is the "wagging mode" at 640 cm^{-1}. According to Table 1 the rolling (ir active) and twisting (ir inactive) modes of SiH_2 are supposed to occur at the same frequency, a fact that seems to be borne out by the experiment. As will be discussed in Section 3.4, the area of this ir band can be used to measure the hydrogen concentration. In Raman the corresponding peak is usually observed at $\approx 660\ cm^{-1}$ a fact which may reflect that the Raman measurements are usually performed on heavily hydrogenated samples for which the solid state down-shift may be smaller (conversely, the rolling and/or twisting modes of SiH_2 may occur at slightly higher frequency than the wagging mode of SiH). We note that the structure sometimes reported at $\approx 600\ cm^{-1}$ (Fig. 10 of [2]) is usually due to two-phonon absorption in the c-Si substrate.

We discuss next the bond bending bands in the 840 to 900 cm^{-1} region. In some relatively weakly hydrogenated samples (≈ 5 to 10%), and depending on preparation conditions, a single peak at 875 cm^{-1} is seen. It corresponds to the single A_1 bending mode of SiH_2 (Table 1). For higher H concentrations usually two peaks are seen, one at 840 cm^{-1} and the other at 890 cm^{-1}. The ratio of intensities of these peaks varies with preparation conditions although for certain sets of parameters it is possible to obtain a constant ratio independent of H concentration (see Fig. 1 of [6]). The 840 cm^{-1} peak can become stronger than that at 890 cm^{-1} at high H concentrations (Fig. 9 of [2]). The interpretation of this doublet poses some difficulties as the samples under consideration show no traces of SiH_3 bonds in their bond stretching spectrum (for SiH_3 an A_1–E bond bending doublet is expected, see Table 1). The doublet under consideration was tentatively interpreted in [32] as due to interaction between bending modes in $(SiH_2)_n$ polymer chains. It was reinterpreted in [4] by analogy to the spectra of polyethylene and polypropylene which exhibit doublets at 1450 to 1365 cm^{-1}, a region which for the C–H bond is equivalent to the 840 to 900 cm^{-1} region of the S–H bond.

Within this interpretation the 890 cm^{-1} peak would be due to the bending mode, while the 840 cm^{-1} peak would be a rolling or a twisting mode. This assignment is incompatible with the predictions of Table 1 and therefore we proceed to reexamine it. First of all we note that the lower frequency component of the polyethylene doublet contains a strong admixture of the skeletal C–C vibrations [34] which, for carbon, occur in the same region. This is not the case for silicon. For polypropylene the doublet contains also a strong admixture of $CH–CH_2$ angular vibrations. We thus feel compelled to return to the original interpretation involving interactions between neighboring SiH_2 groups. The spectra of cyclic $(SiH_2)_5$ and $(SiH_2)_6$ show splittings in the 840 to 900 cm^{-1} region, of the type required to explain the doublet under consideration [26, 27]. In $(SiH_2)_6$, for instance, there is a doublet in the ir spectrum at 900 and 865 cm^{-1}, the upper component being Raman active but not the lower. This is precisely the type of behavior exhibited by the doublet under consideration (see Fig. 6 in [4]). We thus postulate that the doublet seen in a-Si at 840 to 890 cm^{-1} is due to the interaction between two SiH_2 groups attached to nearest neighbor Si atoms in "cis" (same side with repect to Si rings) configuration similar to that of the cyclosilanes. We note that the Raman active upper component of the doublet shows a depolarized Raman spectrum [52]. This favors its assignment to the asymmetric (or more asymmetric) component of the $(SiH_2)_2$ grouping. The lower frequency component, nearly Raman inactive (see Fig. 6 of [4]) would then be the symmetric component.

We discuss next the bending modes of SiH_3 groupings. They produce a distinct doublet with nearly the same splitting but at slightly higher frequency (920 to 860 cm^{-1}) than the one just discussed (see Fig. 5 of [4]). In view of the data in Table 1 we assign the 920 cm^{-1} component to the asymmetric (E) mode and the 860 cm^{-1} one to the symmetric (A_1) mode. We note that only the E-mode shows Raman activity [4] although the A_1 mode is also Raman allowed by symmetry.

While most of the modes in Table 1 have been observed in a-Si–H, there remain a few which have not. They are the rocking (B_1) mode of SiH_2, which should be around 400 cm^{-1}, the wagging (E) and the twisting (A_2) modes of SiH_3. The rocking (B_1) mode

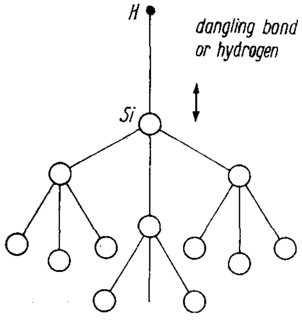

Fig. 4. Schematic diagram of the vibrations leading to the 210 cm^{-1} peak in the infrared (and Raman) spectra of a-Si:H

of SiH_2 should be weak in infrared absorption for geometric reasons and also according to [27]. Besides, it should be degenerate with the vibrations of the Si–Si matrix which may shift it and smear it out. For similar reasons the wagging (E) mode of SiH_3 may not have been observed (the total amount of SiH_3 groups present is never too large). The twisting mode of SiH_3 ($\approx 100\ \mathrm{cm}^{-1}$ according to Table 1) is neither Raman nor ir active.

We mention before closing this section the peak observed at $210\ \mathrm{cm}^{-1}$ in ir [16] and Raman [19, 36] spectra. This peak, which is quite strong and relatively sharp in the ir spectrum, occurs at the upper edge of the TA phonon band. Although it is roughly linear in hydrogen concentration it shows only a very small shift ($\approx 5\ \mathrm{cm}^{-1}$) upon deuteration [37]. Hence the corresponding mode must involve mainly vibrations of *silicon* atoms. Nevertheless the mode is induced by the presence of hydrogen [16]. We point out that this mode is very weak in the Raman spectra [19, 36] while it appears very strong in the ir, a fact which must be due to the circumstance that the undistorted Si–Si bond is not infrared active. The $210\ \mathrm{cm}^{-1}$ peak appears strongly over the weakly allowed (through band distortions) ir absorption of the Si–Si network.

Three seemingly different, but possibly related interpretations of this structure have been given [16, 19, 20]. In [16] the structure was related to the substitutional mass defect mode which appears, for instance, in B-doped c-Si [38]. This structure arises from the sharp, step-like singularity in the density of states of c-Si at the top of the TA band. It is questionable whether the model is applicable to non-substitutional hydrogen, and there is no reason why the density of states singularity should remain as sharp in a-Si as in c-Si. It is therefore preferable to use a localized picture to describe these vibrations, along the lines followed in [19].

We thus consider the vibrations of the unit of Fig. 4 in which the upper Si, tied to a hydrogen atom, moves together with the hydrogen and the rest of the system, for the time being, is assumed not to move. The frequency of this "vibration" can be easily found to be given by

$$\omega^2 \approx M^{-1}3^{-1}(f_{rr} + 8f_{cc} + 3.3f_{BB}) , \tag{11}$$

where f_{rr} is the force constant for the stretching of the Si–Si bond and f_{cc} the angular force constant for Si–Si–Si bonds. From [39] we find $f_{rr} = 1.4 \times 10^5$ dyn/cm and $f_{cc} = 0.9 \times 10^4$ dyn/cm. Another estimate of f_{cc} is possible by fitting the $\omega_{TA}(X)$ and $\omega_{TO}(X)$ frequencies with the formulas [40]

$$\omega_{TA}^2\omega(X) \approx 12f_{cc} , \qquad M\omega_{TA}^2(L) \approx 6f_{cc} .$$

We obtain in this manner $f_{cc} \approx 3.3 \times 10^3$ dyn/cm, nearly three times smaller than the estimate above based on a fit of the elastic constants. In spite of these discrepancies we believe that it is more reasonable to take a value of f_{cc} derived from TA frequencies at the edge of the zone to describe local modes which will turn out to be localized near those modes. With $f_{BB} = 1.86 \times 10^4$ dyn/cm (Section 2.2) and the other parameters just given we find from (11) $\omega = 213\ \mathrm{cm}^{-1}$. This vibration at $\omega = 213\ \mathrm{cm}^{-1}$ is actually not an eigenstate of the system as it is coupled to a partly overlapping continuum. The continuum, however, is very weak at $213\ \mathrm{cm}^{-1}$ and the coupling is expected to be small. Hence a *sharp* resonance or quasi-bound vibrational state is expected at $\approx 213\ \mathrm{cm}^{-1}$, in agreement with experiment ($\approx 210\ \mathrm{cm}^{-1}$).

We note that (11) can also be used to estimate the vibrational frequency of Fig. 4 with a dangling bond instead of the hydrogen atom. In this case f_{BB} would be expected to be smaller than for a saturated bond. For the extreme case $f_{BB} = 0$ we find $\omega = 182\ \mathrm{cm}^{-1}$. This frequency lies quite far into the TA background and will, most probably, not lead to a quasi-bound state or sharp resonance. Hence, pending a more quantitative type of calculation, we conjecture that the presence of dangling bonds saturated by hydrogen or deuterium, and not simply of unsaturated dangling bonds, is necessary for the observation of the quasi-bound state at $\approx 210\ \mathrm{cm}^{-1}$.

We point out that in [20] the frequency under consideration appears as a surface mode of a series of units of the type of Fig. 4 placed on a [111] surface of c-Si. The main contribution to the surface mode arises form the edge of the surface Brillouin zone. This mode could become ir active inspite of being an edge-of-zone mode, through disorder or through curling of the surface in a spherical void. Whether a single unit of the type of Fig. 4 or a two-dimensional array is required to produce the quasi-bound state remains an open question. In view of our discussion above we tend to believe that a simple unit suffices.

3.3 c-Si

Hydrogen in c-Si is believed to be able to occupy a number of interstitial and substitutional (i.e. saturating dangling bonds) positions, the latter related to single and multiple vacancies [41]. A theoretical evaluation of some of the corresponding vibrational frequencies has been given in [41]. A detailed quantitative correlation between interstitial positions and the large number of observed ir absorption peaks [10 to 15] has, so far, not been found although some of these positions have been invoked in [11] to explain some of the observed vibrational frequencies. In [12], however, the interpretation follows the lines of this paper and includes only hydrogen bonded to dangling Si bonds. The variety of bond stretching lines observed in the 1830 to 2220 cm^{-1} region are interpretated in terms of SiH, $\mathrm{SiH_2}$, and $\mathrm{SiH_3}$ groups (SiH_n) with the Si attached to a number (0 to $4 - n$) of dangling bond or impurity atoms (carbon, oxygen). In [12] the assignment of the observed bond stretching frequencies is helped by a detailed study of the annealing behavior of the corresponding absorption peaks.

The peak at 1980 to 1990 cm^{-1} is assigned in [12] to (SiSiSi)Si–H bond stretching vibrations (one Si bond attached to H, the other three to Si). This mode would correspond to the bulk mode of Si–H in a-Si. It must therefore incorporate the "solid state effect" discussed in Section 3.2, i.e., it must correspond to Si–H bonds pointing toward a Si vacancy. However, this band anneals away at ≈ 300 °C while the corresponding band in a-Si anneals away at 500 °C [5]. An explanation for the different behavior may be the presence of *pairs* of Si–H pointing towards the vacancy in c-Si and only single Si–H in a-Si. The pairs would evolve as $\mathrm{H_2}$ molecules and then would be expected to anneal away at lower temperatures than for a-Si. We point out that the peak reported at 1968 cm^{-1} in [11], probably equivalent of the one just discussed, anneals away at 600 °C. Similarly, a shoulder at $\approx 2000\ \mathrm{cm}^{-1}$ is seen in Fig. 2 of [10] for c-Si after annealing to 400 °C.

Two peaks observed at 1890 and 1930 cm^{-1} are assigned in [12] to (Sidd)Si–H and (SiSid)Si–H groups, respectively, where d represents a dangling bond. The downshift in frequency with respect to the (SiSiSi)Si–H peak can be accounted for by postulating that the dangling bond has zero electronegativity.

The peak at ≈ 2060 assigned in [12] to (SiSi)$\mathrm{SiH_2}$ falls well into the scheme of this paper. In [12] it is suggested that the $\mathrm{SiH_2}$ groups are in the inner surface of a divacancy (see Fig. 5b of [12]). In such a situation a "solid state" down-shift of $\approx 60\ \mathrm{cm}^{-1}$, required to bring this frequency into agreement with the corresponding one in Table 1 (2128 cm^{-1}) can be easily accounted for. The peaks seen at 2083 and 2107 cm^{-1} for c-Si (2985 and 2105 cm^{-1} in [10]) are accounted for in [12] as due to (CCSi)SiH and (CSi)$\mathrm{SiH_2}$ group. We find the CC clustering of the residual carbon impurity to be somewhat unpalatable and prefer an assignment to (SiSi)$\mathrm{SiH_2}$ groups at the inner surfaces of larger voids (the 2107 peak), so as to agree with the peak of a-Si at 2100,

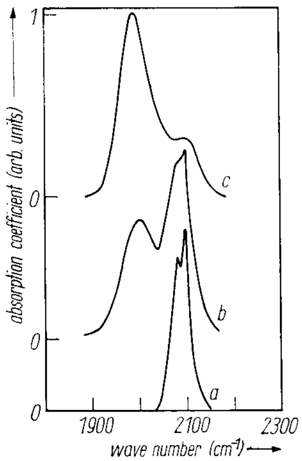

Fig. 5. Bond stretching ir absorption spectra of microcrystalline (2.5%) and mixed microcrystalline–amorphous Si–H [53]. $[SiH_4]/([H_2]+[SiH_4]) = 2.5$ (a), 5 (b) and 10% (c)

and with (SiSiS)SiH in a similar situation (the 2083 cm^{-1} peak). The latter would agree with the peak observed for SiH at [111] surfaces of c-Si (Section 3.2). We point out, however, that the presence of SiH_2 groups should be accompanied by bond bending bands in the 840 to 900 cm^{-1} region. No mention of the presence or absence of these bands is made in [10 to 12]. Recent work by Richter [53] has shown two infrared absorption peaks at 2085 and 2100 cm^{-1} in microcrystalline samples obtained by the plasma transport (Vepřek) technique (see Fig. 5). In this case no trace of the bond bending modes was seen. The most likely explanation of the two bond stretching peaks, which must be related to Si–H bonds, is that they correspond to Si–H bonds on two different crystallographic surfaces, possibly (111) and (110). In Fig. 5 we see clearly that the Si–H stretching peaks of the crystalline samples (labelled 2.5%) are much narrower than those of the amorphous material (labelled 10%).

The assignment of a peak at 2160 cm^{-1} (c-Si) in [12] to $(OSi)SiH_2$ agrees reasonably with a similar structure observed at 2180 cm^{-1} in a-Si in [2]. In this reference a peak at 2240 cm^{-1} (oxygenated a-Si) is attributed to $(OO)SiH_2$. It may also be related to the 2210 to 2218 cm^{-1} peak attributed in [12] to $(OC)SiH_2$.

The structure seen in [10] at 2135 to 2155 cm^{-1} could be related to the A and E stretching modes of $(Si)SiH_3$ groups (see Table 1). An alternative possibility is SiH_3 groups attached to distinct crystallographic surfaces, such as (111) and (110).

The bond wagging (rolling) modes of c-Si(H) are also reflected in an absorption peak at ≈ 640 cm^{-1} [10 to 12]. This peak may have some substructure but, in our opinion, it is not possible to disentangle it as it overlaps the two-phonon absorption peaks of c-Si (≈ 610 cm^{-1}). Overlap with somewhat weaker two-phonon bands of c-Si also occurs in the 800 to 900 cm^{-1} region. There seems, however, to be a peak in this region at ≈ 890 cm^{-1} related to the presence of (SiH_2) groups.

3.4 Absorption strength

A discussion of the integrated strength of the ir absorption bands due to SiH bonds in a-Si is required in order to extract from the measured spectra information on the concentration of the various SiH groups present. The starting point for an interpretation of this integrated strength is the Lorentzian expression [2],

$$\Delta\varepsilon(\omega) = (4\pi N e_s^{*2} m^{-1})/(\omega_0^2 - \omega^2 - i\omega\gamma)\,, \qquad (12)$$

where $\Delta\varepsilon(\omega)$ represents the contribution of one bond to the dielectric constant of the vibrational mode, ω_0 its frequency, γ the damping constant, e_s^* an effective dynamical charge of the bond in the solid (i.e. the derivative of the induced dipole moment with respect to the displacement of the H atom), and N the density of Si–H bonds. By integrating the imaginary part of $\omega\,\Delta\varepsilon$ and using (11) we obtain

$$N_H = [1/(2\pi^2)]\,[m/(e_s^{*2})] \int \omega\, \mathrm{Im}\, \Delta\varepsilon\, d\omega = [(cn/2\pi^2)]\,[m/(e_s^{*2})] \int \alpha(\omega)\, d\omega\,. \tag{13}$$

In (13) α is the absorption coefficient and n the real part of the refractive index. In order to obtain from the integral of $\alpha(\omega)$ the bond density N_H we must know the effective charge e_s^*. Ideally we would like to relate e_s^* to the corresponding quantity in gaseous silanes e_G^*. However, in the solid a-Si:H e_G^* is modified by local field effects and by screening by the a-Si matrix. There may also be a direct modification of the dipole moment of the Si–H bond. The task of evaluating e_s^* from e_G^* is therefore rather hopeless. Nevertheless several attempts have been made, using simple electrostatic models [1, 2] which we discuss below. The absorption strength of a molecular vibration in gases is often given in terms of the parameter Γ related to the effective charge e_G^* through

$$e_G^{*2} = ([c\omega_0 m]/[2\pi^2 N_A])\,(\Gamma/\xi)\,, \tag{14}$$

where N_A is Avogadro's number and ξ the number of bonds contributing to the vibrational band under consideration; Γ is usually found in cm^2/mmol.

Equation (13) can be rewritten as

$$N_H = A \int \omega^{-1} \alpha(\omega)\, d\omega\,, \tag{15}$$

where the integral is extended to only one of the absorption modes and A is usually given in cm^{-2}. The constant A is thus related to e_s^* through

$$A(\mathrm{cm}^{-2}) = (cnm\omega_0)/(2\pi^2 e_s^{*2}) = 0.7\omega_0(\mathrm{cm}^{-1})\, e_s^{*-2}(\text{at. units}) \times 10^{16}\,. \tag{16}$$

Table 4

Parameter A which relates the strength of the infrared bands of a-Si:H and a-Ge:H to the hydrogen concentration (from [6] and [47])

a-Si:H	640 cm^{-1}	840 to 890 cm^{-1}	2000 cm^{-1}	2100 cm^{-1}	2100 cm^{-1}
	wag SiH roll SiH$_2$	bend*) SiH$_2$ SiH$_3$	stretch SiH	stretch SiH	stretch SiH$_2$
A (10^{17} cm^{-1})	1.6	2.0	2.2	17	9.1
a-Ge:H	565 cm^{-1}		1895 cm^{-1}	1970 cm^{-1}	
	wag SiH roll SiH$_2$		stretch SiH	stretch SiH–SiH$_2$	
A (10^{19} cm^{-1})	1.1		≈ 5	≈ 14	

*) For samples with a 890 cm^{-1} peak twice as strong as the 840 cm^{-1} one. A decreases if the relative strength of the 840 cm^{-1} peak increases.

In (16) we have assumed $n \approx 3.4$. It can be somewhat smaller in heavily hydrogenated samples. The values of A for some of the modes observed in a-Si:H are listed in Table 4. They were obtained by measuring the integrated ir absorption of the corresponding bands for samples whose hydrogen concentration had been determined independently by measuring the total amount of hydrogen effused upon annealing or by the nuclear reactions technique [5, 6, 42, 43]. We should point out that the separation of the 2100 cm^{-1} band into SiH and SiH_2 is rather inaccurate. It is based on samples which show only a 2100 cm^{-1} stretching band and no bond bending band (800 to 900 cm^{-1} region). The strength of the 2100 cm^{-1} band in these samples is rather weak (see Fig. 1 of [6]) and hence the separation cannot be made very precisely. By the same token, the accuracy in the determination of the constant A for the bond bending modes cannot be very high since it is based on removing from the 2100 cm^{-1} band the component not related to SiH_2. Also, it has been recently shown [44] that the strength of the 840 cm^{-1} component of the bending bands can be reversibly changed by means of Ar-ion bombardment without changing either the strength of the 890 cm^{-1} component or the hydrogen concentration. Hence it seems that the strength of the 840 cm^{-1} absorption depends critically on changes in local fields produced by the change in local environment associated with the argon bombardment. In glow discharge samples containing as much as 30% of $H(Si_2H)$ the constant A of the bending modes decreases by approximately a factor of 3, corresponding to an increase of ≈ 1.7 in the dynamic charge of the mode [45].

The three different A's involved in the bond stretching vibrations (Table 4) lead to a *total* strength of these bands which is not proportional to the hydrogen concentration. From (16) and the data of Table 4 we obtain the dynamical charges (in units of the elementary charge e)

$$e_s^*(2000) = 0.8; \qquad e_s^*(2100, \text{SiH}) = 0.29; \qquad e_s^*(2100, \text{SiH}_2) = 0.40 . \tag{17}$$

From the stretching mode of mono- and polysilanes [2] we obtain with (14) $e_G^* = 0.16$. It remains now to discuss possible mechanisms which can enhance the charge e_G^* up to the values of (17). If one assumes that the Si–H bonds are placed inside of a spherical cavity one obtains as a result of the local field enhancement [2]

$$e_s^* = [3\varepsilon/(1 + 2\varepsilon)]\, e_G^* \approx (3/2) e_G^* , \tag{18}$$

where $\varepsilon \approx 12$ is the dielectric constant of the Si matrix. Equation (18) can account for the type of enhancement found for the 2100 cm^{-1} band. The charge of the 2000 cm^{-1} band seems too large to be obtained by this mechanism. We note that the Szigetti-type correction suggested by Connell and Pawlick [1]

$$e_s^* = (1/3)\,(\varepsilon + 2)\, e_G^* \tag{19}$$

gives a charge $e_s^* = 0.76$ close to that for the 2000 cm^{-1} peak. While interesting, we consider this result to be fortuitous. The Clausius-Mossotti local field is known not to be appropriate to the electronic polarizability of Si [46]. It is, in principle, possible to increase the local field enhancement of (18) by using an oblate ellipsoidal cavity The difficulty with this interpretation would be in the effective charge associated with the wagging modes, for which the local field enhancement would decrease. From the Γ's of Table 4 of [2] we obtain for the wagging mode $e_G^* = 0.1$. The value of e_s^* corresponding to the A of Table 4 for this mode (equation ((16)) is $e_s^* = 0.53$. The local field correction required to bring this e_s^* into agreement with e_G^* is also much larger than that of the spherical cavity (equation (18)). If we make the cavity oblate ellipsoidal, so as to explain the A of the 2000 cm^{-1} stretching mode, the local field correction of the wagging mode would decrease. We thus have to regard the large oscillator strengths as unexplained. They are probably due, in part, to a direct modification of. the dipole moment of the Si–H bond in the solid.

We mention that the strength of the 2000 cm^{-1} bond stretching band saturates with increasing H concentration at a level of 3×10^{21} atoms/cm^3 (6% of hydrogen) [6]. This seems to represent a solubility limit of the hydrogen in the bulk of the semiconductor. The 2100 peak continues to increase up to a level of $\approx 30\%$ hydrogen (Si_2H) for samples prepared on room temperature substrates or above room temperature. At these temperatures it is usually not possible to introduce more hydrogen in the samples. For glow discharge samples prepared on substrates below room temperature, higher H concentrations are possible [4].

It has been pointed out [5, 6, 43] that the integrated strength of the bond wagging absorption peak is quite accurately proportional to the total hydrogen concentration and that, once the corresponding A is known (Table 4), it can be used to determine this concentration. This conclusion holds for samples containing SiH and SiH_2 groups in variable proportions. Samples with large amounts of SiH_3 groups have not been investigated. It is unlikely that this conclusion will hold for these samples as the wagging modes of SiH_3 should, according to Table 1, be shifted down to about 500 cm^{-1}. A decrease in the strength of the 640 cm^{-1} with respect to the stretching modes has been seen for samples with the composition $SiH_{1.5}$, containing large amounts of SiH_3 groups [45] but we have seen no evidence of the 500 cm^{-1} wagging mode. Thus their oscillator strength must be weak. We note that according to [30] the E wagging bands in disilane ($\approx$ 380 cm^{-1}) are *four times weaker* than the E bending bands. The wagging band of SiH_3 is expected to overlap with the vibrations of the Si–Si matrix and, if weak, should be difficult to disentangle from it.

If we assume that the band at 640 cm^{-1} contains both, the wagging vibrations of SiH and the rolling vibrations of SiH_2, we must assume that the latter are about twice as strong as the former per hydrogen bond involved in order to account for the proportionality of their strength to the H concentration: There is only one rolling mode of SiH_2 for each SiH_2 group (i.e., for a pair of H atoms). We thus conclude that the strengths of the infrared absorption are difficult to explain in detail theoretically. The empirical rules given above and in Table 4 should, however, be useful for the characterization of a-Si(H) when used with due care.

4. Vibrational Spectra of a-GeH$_n$

4.1 Vibrational frequencies

The vibrational spectrum of a-Ge:H has not been studied as intensively as that of a-Si:H. Infrared studies were published in [1, 4, 8, and 16]. Raman studies appeared in [36]. No systematic studies of c-Ge have appeared. These spectra seem to be very similar to those of a-Si, with the corresponding force constants slightly reduced for Ge as a result of the slightly larger bond length (see Table 5 here and Table 2 in [8]). The stretching modes also show two components, one at 1970 cm^{-1} and the other at 1895 cm^{-1}. The interpretation parallels that for silicon: the 1970 cm^{-1} component is due to GeH_2 groupings and to GeH inside of cavities much larger than that which corresponds to a monovacancy (see Fig. 2 of [8] where the 1970 cm^{-1} peak increases upon annealing while the bending peaks disappear). The 1895 cm^{-1} component corresponds to GeH in a cavity of the size of the monovacancy. The latter component also saturates for a bond concentration $\approx 5\%$ (see Fig. 4 of [1]). Some evidence for GeH_3 stretching vibrations is seen at 2060 cm^{-1}.

The split bending modes of neighboring GeH_2 groups appear at 755 to 820 cm^{-1}. For a sample with a considerable amount of GeH_3 groups (Fig. 9 of [4]) these peaks shift to 770 and 830 cm^{-1}, possibly as a result of the appearance of the bond bending structure of GeH_3. The wag (GeH)–roll (GeH_2) mode appears at 565 cm^{-1} and the low

Table 5

Vibrational frequencies (in cm^{-1}) of structures observed in the infrared and Raman spectra of a-Ge:H related to the presence of hydrogen

	GeH	GeH_2	GeH_3
bond stretching	1895 (E)	1975 (A_1) 1970 (B_1)	2060 (A_1, E)
bond bending	—	820 $(GeH_2)_2$ 755	830 E 770 A_1
wag, roll	565 (E)	565 (B_2)	
rock		≈ 400 ? (B_1)	
Ge_3–GeH	120	120	

frequency quasi-local mode, which corresponds to the 210 cm^{-1} vibration of a-Si:H, at 120 cm^{-1}. There is some evidence for the rocking mode at ≈ 400 cm^{-1} in Fig. 2 and 3 of [8].

4.2 IR-absorption strength

The absorption strengths as a function of hydrogen concentration have been investigated in [47]. This work, however, was not as thorough as that of [6] for a-Si. The strength of the wagging–rolling modes 565 cm^{-1} is proportional to the hydrogen concentration, the constant A being

$$A_w(\mathrm{Ge}) = 1.1 \times 10^{19}\ \mathrm{cm}^{-2}\,. \tag{20}$$

The strength of the stretching modes is not proportional to the hydrogen concentration (see Fig. 2 of [47]). A decomposition into separate A-constants for the 1975 cm^{-1} and the 1895 cm^{-1} peaks has not been made. We try to extract approximate values of these constants from Fig. 2 of [47] by assuming that the low pressure region in this figure corresponds mainly to the 1895 cm^{-1} peak while the high pressure region contains mainly the 1975 cm^{-1} peak. We obtain in this manner the tentative values listed in Table 4. We note that, also in this case, the effective charges obtained from these A-values with (16) are much larger than those found by applying to the e^*_G's of GeH_4 [48] the local field correction of (17).

5. Recent Developments

In a recent paper Azoulay et al. [49] have performed EXAFS (extended X-ray absorption fine structure) on two samples of a-Ge:H with 4.5 and 6 at% H. They can determine changes in effective coordination number and in bond length. Their data can be explained by assuming that about 1.5% of the hydrogen replaces Ge vacancies while the rest is bound to microvoid surfaces. This picture agrees with the one given here, although the concentration of 1.5%, representing a bulk solubility limit, is somewhat smaller than that suggested here and elsewhere [1] for Si (5%). We note that nuclear resonance experiments also suggest the existence of two types of bonded hydrogen [6, 50], one responsible for a narrow NMR line and another responsible for a broad line. The narrow line variety saturates at ≈ 3 at% H concentrations and could well correspond to our H dissolved in the bulk, which gives rise to the 2000 cm^{-1} bond stretching band. The broad NMR line species would be that lining up surfaces of voids.

Very recently Kamitakahara [54] has succeeded in measuring the inelastic scattering spectrum of thermal neutrons produced by pure and hydrogenated ($\approx$ 10 at%) a-Si. The pure spectrum yields the exact density of states for Si–Si vibrations while the hydrogenated sample yields, to a good approximation, the spectral function for the H motion (the scattering cross section of H is $\approx$ 50 times that of Si). This author was able to see the 210 cm^{-1} quasi-local mode which appears in the scattering spectrum of a-Si:H considerably stronger (one to two orders of magnitude) above the background than for the Raman spectrum [36]. This is reasonable as the Raman spectrum contains both the Si–H and the Si–Si vibrations while the neutron spectrum contains only the motion of the hydrogen. The quasi-local mode, however, is stronger in the ir than in the neutron spectrum (a factor of 2 to 3 relative to the TA background). This means that the dynamic charge related to the quasi-local mode is larger than that for the background. We estimate for the local mode a dynamical charge of $\approx 0.6e$. A theoretical study of local mode will soon appear [55].

Acknowledgements

I would like to thank the Xerox Palo Alto Research Centers for an appointment as visiting scientist while this work was being written up. Thanks are also due to J. Knights, R. J. Nemanich, J. Boyce, and R. M. Martin for a number of fruitful discussions, and for making their data available to me while writing this work.

References

[1] G. A. N. CONNELL and J. R. PAWLIK, Phys. Rev. B **13**, 787 (1976).
[2] M. H. BRODSKY, M. CARDONA, and J. J. CUOMO, Phys. Rev. B **16**, 3556 (1977).
[3] C. C. TSAI, H. FRITZSCHE, M. H. TANIELIAN, P. J. GACZI, D. D. PERSANS, and M. A. VESAGHI, in: Amorphous and Liquid Semiconductors, Ed. W. E. SPEAR, Univ. Edinburgh, 1978 (p. 339).
[4] G. LUCOVSKY, R. J. NEMANICH, and J. C. KNIGHTS, Phys. Rev. B **19**, 2064 (1979).
J. C. KNIGHTS and G. LUCOVSKY, Crit. Rev. Solid State Sci. **9**, 210 (1980).
[5] H. SHANKS, C. J. FANG, L. LEY, M. CARDONA, F. J. DEMOND, and S. KALBITZER, phys. stat. sol. (b) **100**, 43 (1980).
[6] H. R. SHANKS, F. R. JEFFREY, and M. E. LOWRY, J. Physique **42**, C4-773 (1981).
[7] P. JOHN, I. M. ODEH, M. J. K. THOMAS, M. J. TRICKER, D. MCGILL, A. WALLACE, and J. I. B. WILSON, J. non-crystall. Solids **35–36**, 237 (1980).
[8] D. BERMEJO and M. CARDONA, J. non-crystall. Solids **32**, 421 (1979).
[9] H. WAGNER, R. BUTZ, U. BACKES, and D. BRUCHMANN, Solid State Commun. **38**, 1155 (1981).
G. E. BECKER and G. W. GOBELI, J. chem. Phys. **38**, 2942 (1963).
[10] A. HIRAKI, T. IMURA, K. MOGI, and M. TASHIRO, J. Physique **42**, C4-277 (1981).
[11] B. N. MUKASHEV, K. H. NUSSUPOV, M. F. TAMENDAROV, and V. V. FROLOV, Phys. Letters A **87**, 376 (1982).
[12] T. S. SHI, S. N. SAHU, G. S. OEHRLEIN, A. HIRAKI, and J. W. CORBETT, phys. stat. sol., to be published.
[13] H. J. STEIN, Phys. Rev. Letters **43**, 1030 (1979).
[14] N. N. GERASIMENKO, M. ROLLÉ, LI-JEN CHENG, Y. H. LEE, J. C. CORELLI, and J. W. CORBETT, phys. stat. sol. (b) **90**, 689 (1978).
[15] CUI SHU-FAN, GE PEI-WEN, ZHAO YA-QIN, and WA LAN-SHENG, Acta Physica Sinica **25**, 791 (1979).
[16] S. C. SHEN, C. J. FANG, M. CARDONA, and L. GENZEL, Phys. Rev. B **22**, 2913 (1980).
[17] J. E. SMITH, Jr., M. H. BRODSKY, B. L. CROWDER, M. I. NATHAN, and A. PINCZUK, Phys. Rev. Letters **26**, 642 (1971).
[18] M. H. BRODSKY and A. LURIO, Phys. Rev. B **9**, 1646 (1974).
[19] C. C. TSAI and R. J. NEMANICH, J. non-crystall. Solids, **35–36**, 1203 (1980).
[20] E. MARTINEZ and F. YNDURAIN, Solid State Commun. **44**, 1477 (1982).
[21] W. PAUL, Solid State Commun. **34**, 283 (1980).

[22] E. A. Clark and A. Weber, J. chem. Phys. **45**, 1759 (1966).
[23] G. Herzberg, Infrared and Raman Spectra of Polyatomic Molecules, Van Nostrand, New York 1945.
C. W. F. T. Pistorius, J. chem. Phys. **27**, 965 (1957).
K. Venkateswarlu and S. Sundaram, J. chem. Phys. **23**, 2365 (1955).
[24] D. C. McKean, and A. A. Chalmers, Spectrochim. Acta **23A**, 2405 (1967).
[25] L. J. Bellamy, The Infrared Spectra of Complex Molecules, Chapman and Hall, London 1975 (p. 380).
[26] E. Hengge and G. Banner, Angew. Chem. – Internat. Ed. **12**, 316 (1973).
[27] K. Hassler, E. Hengge, and D. Kovar, Spectrochim. Acta **34A**, 1193 (1978).
[28] G. Lucovsky, Solid State Commun. **29**, 571 (1979).
[29] S. N. Sahu, T. S. Shi, P. W. Ge, A. Hiraki, T. Imura, M. Tashiro, V. A. Singh, and J. W. Corbett, J. chem. Phys., to be published.
[30] G. W. Bethke and M. K. Wilson, J. chem. Phys. **26**, 1107 (1957).
[31] H. Wieder, M. Cardona, and C. R. Guarnieri, phys. stat. sol. (a) **74**, 329 (1982).
[32] J. C. Knights, G. Lucovsky, and R. J. Nemanich, Phil. Mag. B **37**, 467 (1978).
J. C. Knights, R. A. Street, and G. Lucovsky, J. non-crystall. Solids **35**–**36**, 279 (1980).
[33] D. Dellafera, R. Labusch, and H. H. Roscher, Phil. Mag. B **45**, 607 (1982).
[34] R. G. Snyder and J. H. Schachtschneider, Spectrochim. Acta **21**, 169 (1965).
[35] H. Tadokoro, M. Kobayashi, M. Ukita, K. Yasufuku, and S. Murahashi, J. chem. Phys. **42**, 1435 (1965).
[36] D. Bermejo and M. Cardona, J. non-crystall. Solids **32**, 405 (1979).
[37] S. C. Shen, C. J. Fang, and M. Cardona, phys. stat. sol. (b) **101**, 451 (1980).
[38] M. Cardona, S. C. Shen, and S. P. Varma, Phys. Rev. B **23**, 5329 (1981).
[39] R. M. Martin, Phys. Rev. B **1**, 4005 (1970).
[40] R. Tubino and L. Piseri, J. Phys. C **13**, 1197 (1980).
[41] Vijay A. Singh, C. Weigel, J. W. Corbett, and L. M. Roth, phys. stat. sol. (b) **81**, 637 (1977).
[42] P. John, I. M. Odeh, M. J. K. Thomas, M. J. Tricker, and J. I. B. Wilson, phys. stat. sol. (b) **105**, 499 (1981).
[43] P. John, I. M. Odeh, M. J. K. Thomas, M. J. Tricker, J. I. B. Wilson, J. B. A. England, and D. Newton, J. Phys. C **14**, 309 (1981).
[44] S. Oguz, D. A. Anderson, and W. Paul, Phys. Rev. B **22**, 880 (1980).
[45] J. Knights and R. J. Nemanich, private communication.
[46] W. Hanke and L. J. Sham, Phys. Rev. B **21**, 4556 (1980).
[47] C. J. Fang, K. J. Grunz, L. Ley, M. Cardona, F. J. Demond, G. Müller, and S. Kalbitzer, J. non-crystall. Solids **35**–**36**, 255 (1980).
[48] I. W. Levin, J. chem. Phys. **42**, 1244 (1965).
[49] Y. Azoulay, C. E. Boulden, E. A. Stern, and B. von Roedern, to be published.
[50] J. A. Reimer, R. W. Vaughan, and J. C. Knights, Phys. Rev. Letters **44**, 193 (1980).
[51] R. S. Armstrong and R. J. H. Clark, J. Chem. Soc., Faraday Trans. II **72**, 11 (1976).
[52] R. J. Nemanich, private communication.
[53] H. Richter, to be published.
[54] J. Kamitakahara, private communication.
[55] E. Martínez and M. Cardona, Phys. Rev., in the press.

(Received October 22, 1982)